

This is a repository copy of *1H, 13C, 15N backbone resonance assignments of the apo and holo forms of the ABC transporter solute binding protein PiuA from Streptococcus pneumoniae*.

White Rose Research Online URL for this paper:

<https://eprints.whiterose.ac.uk/id/eprint/164250/>

Version: Accepted Version

Article:

Edmonds, Katherine A, Zhang, Yifan, Raines, Daniel J orcid.org/0000-0002-3015-6327 et al. (2 more authors) (2020) 1H, 13C, 15N backbone resonance assignments of the apo and holo forms of the ABC transporter solute binding protein PiuA from Streptococcus pneumoniae. Biomolecular NMR Assignments. ISSN: 1874-270X

<https://doi.org/10.1007/s12104-020-09952-9>

Reuse

Items deposited in White Rose Research Online are protected by copyright, with all rights reserved unless indicated otherwise. They may be downloaded and/or printed for private study, or other acts as permitted by national copyright laws. The publisher or other rights holders may allow further reproduction and re-use of the full text version. This is indicated by the licence information on the White Rose Research Online record for the item.

Takedown

If you consider content in White Rose Research Online to be in breach of UK law, please notify us by emailing eprints@whiterose.ac.uk including the URL of the record and the reason for the withdrawal request.

¹H, ¹³C, ¹⁵N backbone resonance assignments of the apo and holo forms of the ABC transporter solute binding protein PiuA from *Streptococcus pneumoniae*

Authors: Katherine A. Edmonds¹, Yifan Zhang^{1,2,3}, Daniel J. Raines⁴, Anne-K. Duhme-Klair⁴, and David P. Giedroc^{1,3*}

¹Department of Chemistry, Indiana University, Bloomington, Indiana, USA

²Graduate Program in Biochemistry, Indiana University, Bloomington, Indiana, USA

³Department of Molecular and Cellular Biochemistry, Indiana University, Bloomington, Indiana, USA

⁴Department of Chemistry, University of York, Heslington, York, YO10 5DD, UK

*Address correspondence to: David P. Giedroc, email: giedroc@indiana.edu

ORCIDs:

Katherine A. Edmonds: 0000-0002-1282-9858

Yifan Zhang: 0000-0001-7048-1098

Daniel J. Raines: 0000-0002-3015-6327

Anne-K. Duhme-Klair: 0000-0001-6214-2459

David P. Giedroc: 0000-0002-2342-1620

Acknowledgments

This research was supported by US National Institutes of Health grant R35 GM118157 to D.P.G. and UK Engineering and Physical Sciences Research Council grant EP/L024829/1 to A.K.D.K. We thank Dr. Hongwei Wu for technical assistance.

Abstract

Streptococcus pneumoniae is a Gram-positive human pathogen that causes millions of infections worldwide with an increasing occurrence of antibiotic resistance. Iron acquisition is essential for its survival and virulence, especially under host-imposed nutritional immunity. *S. pneumoniae* expresses several ATP-binding cassette (ABC) transporters to facilitate acquisition under iron limitation, including PitABC, PiaABC, and PiuABC. The substrate specificity of PiuABC is not fully established. Herein, we report the backbone ^1H , ^{13}C and ^{15}N resonance assignments of the 31 kDa soluble, extracellular domain of PiuA in the apo form and in complex with Ga(III) and the catechol siderophore-mimic 4-LICAM. These studies provide valuable information for further functional studies of interactions with other proteins, metals, and small molecules.

Keywords

Iron acquisition; ABC transporter; pathogen; catechol; siderophore; *Streptococcus pneumoniae*

Biological context

Streptococcus pneumoniae is an important Gram-positive human pathogen (Lanie et al. 2007; Lynch and Zhanel 2010). Iron (Fe) is essential for its survival and pathogenicity, as it is essential for most living organisms, due to its ability to perform redox reactions and function as a cofactor for many proteins (Andreini et al. 2018). During infection, the host often limits the availability of iron in a process known as nutritional immunity (Hood and Skaar 2012). To respond to iron limitation, various *S. pneumoniae* strains express three different ABC transporters. PitABC, PiaABC, and PiuABC each facilitate iron uptake from different sources and as different Fe(III)-chelate complexes. Transporters such as these commonly recognize iron bound to heme or other small organic molecules, including various classes of siderophores (Zhang et al. 2020). *S. pneumoniae* is not known to endogenously biosynthesize siderophores and thus must rely on Fe piracy to meet nutritional Fe demands (Cheng et al. 2013). Hence, the regulated uptake of siderophore- or other small molecule-Fe(III) complexes produced by other, often competing, bacteria in polymicrobial communities or by the host is foundational to Fe piracy in *S. pneumoniae*.

PiuA is the solute-binding protein (SBP) of the PiuABC transporter. As an extracellular membrane-bound lipoprotein, its role is to recognize and bind a specific Fe(III)-complex and transfer it to the transmembrane subunit of the ABC complex embedded in the cytoplasmic membrane for import into the cell. Like most SBPs known to be involved in iron transport in bacteria, PiuA belongs to class III (cluster A), consisting of two α/β lobes connected by a rigid helical linker, with the ligand binding site in a cleft between the lobes (Delepelaire 2019). Members of this class typically display very little structural rearrangement upon ligand binding (de Boer et al. 2019). This feature leaves some questions as to how substrate binding promotes transport.

Previous nuclear magnetic resonance studies of a similar protein, the *E. coli* FepB, an SBP involved in import of Fe(III) in complex with the siderophore enterobactin, shows that Ga(III) is

a suitable diamagnetic substitute for the paramagnetic Fe(III), enabling detailed structural and dynamic analysis without extensive line-broadening (Chu et al. 2014).

Similarity to the SBPCeuE of *Campylobacter jejuni* predicts that PiuA might also bind coordinately unsaturated iron complexes of tetradentate siderophores and their mimics, for example 4-LICAM, a *bis*-catecholate which contains a four-atom linker between two simple catecholamide units (Raines et al. 2013; Wilde et al. 2017).

Herein, we report the resonance assignments of the backbone ^1H , ^{13}C and ^{15}N atoms of the 31 kDa soluble, extracellular domain of *S. pneumoniae* PiuA in the apo form and in complex with Ga(III) and 4-LICAM, which provide valuable information for further studies of the dynamics and interactions with other proteins, metals, and small molecules.

Methods and experiments

Sample preparation

The region of the gene encoding the soluble, extracellular domain of PiuA, SPD_1652 residues 37-321 was PCR-amplified from the genomic DNA of *S. pneumoniae* D39 strain (Lanie et al. 2007), and inserted into the pSUMO expression vector (Peroutka et al. 2011). Uniformly ^{15}N , ^{13}C , ^2H protein was expressed in *E. coli* BL21 (DE3) cells in M9 minimal medium containing 1 kg D_2O , as well as 1.0 g of $^{15}\text{NH}_4\text{Cl}$ and 2 g $^{13}\text{C}_6,^2\text{H}$ -glucose as the sole nitrogen and carbon sources, respectively. Expression was induced by addition of 1 mM isopropyl β -d-1-thiogalactopyranoside (IPTG) at OD_{600} 0.7 and allowed to continue overnight at 18 °C. Cells were harvested by centrifugation, resuspended in buffer A (25 mM Tris pH 8.0, 500 mM NaCl, 10% glycerol, and 20 mM imidazole), then lysed by sonication on ice. The crude lysate was clarified by centrifugation. 70% ammonium sulfate was added to the soluble fraction, and the precipitated protein was collected by centrifugation, and then resuspended in buffer A. The tagged protein was isolated by Ni(II) affinity chromatography using a 5 mL HisTrap FF column (GE Healthcare Life Sciences) with a gradient from 100% buffer A to 100% buffer B (25 mM Tris pH 8.0, 500 mM NaCl, 10% glycerol, and 500 mM imidazole). Eluted fractions were pooled and cleaved with SUMO protease while dialyzing overnight at room temperature into buffer A supplemented with 2 mM dithiothreitol (DTT). Uncleaved protein, protease, and the SUMO tag were removed by passage through the HisTrap FF column equilibrated in buffer A prior to further purification by size-exclusion chromatography in buffer C (25 mM Tris pH 8.0, 500 mM NaCl, 2 mM ethylenediaminetetraacetic acid [EDTA]), using a Superdex-75 column on an Akta Pure system (GE Healthcare Life Sciences).

To facilitate exchange of deuterated amides back to protons, the purified protein was incubated with 2.5 M guanidinium-HCl and 5 M EDTA for 3 hours, then dialyzed into buffer C and then into NMR buffer (25 mM MES pH 6.5, 150 mM NaCl, treated with Chelex (Biorad)). ^{15}N TROSY spectra on samples labeled with only ^{15}N were used to confirm nearly complete back-exchange of the deuterated sample.

To obtain the holo sample, 4-LICAM, synthesized according to a previously published procedure (Wilde et al. 2013), was dissolved in neat DMSO to a concentration of 30 mM and mixed with

20 mM GaCl₃ in 0.3 M HCl and diluted to a final concentration of 1 mM GaCl₃ in 50 mM HEPES, pH 7.2, 150 mM NaCl. This was used as a stock Ga(III)-4-LICAM complex and added to \approx 3-fold molar excess over [PiuA] in the same buffer, incubated 4 h at RT, and buffer exchanged into NMR buffer using an Amicon ultra centrifugal filter unit (10 kDa cut-off) while removing free ligand.

NMR experiments

NMR samples for backbone assignment contained 0.8-0.9 mM protein, with 25 mM MES pH 6.5, 150 mM NaCl, and 10% v/v D₂O, with 0.3mM 2,2-dimethyl-2-silapentanesulfonic acid (DSS) as an internal reference. NMR spectra were recorded at 35 °C on a 600 MHz Bruker Avance Neo spectrometer equipped with a cryogenic probe in the METACyt Biomolecular NMR Laboratory at Indiana University, Bloomington. Backbone chemical shifts were assigned for each state using TROSY versions of the following standard triple-resonance experiments: HNCACB, HNCOCACB, HNCA, HNCOCACB, HNCO, and HNCACO (Salzmann et al. 1999), using non-uniform sampling with Poisson gap schedules (Hyberts et al. 2010). Data were processed using NMRPipe (Delaglio et al. 1995) and istHMS (Hyberts et al. 2012), and analyzed using CARA (Keller 2004) and Sparky (Lee et al. 2015), all on NMRbox (Maciejewski et al. 2017).

Assignments and data deposition

The soluble, extracellular domain of PiuA consists of 285 residues. Nearly complete backbone assignments were obtained for the apo (ligand-free) and holo [Ga(III)-4-LICAM] forms of PiuA, as shown in the ¹⁵N TROSY spectra in Figure 1 and Figure 2, respectively. Amide proton and nitrogen assignments are missing for R237 and H238 of the apo form, and for R216 and R237 in the holo form. These crosspeaks are missing likely due to line-broadening caused by conformational exchange; the crystal structure of a close homolog (PDB 4JCC) from *S. pneumoniae* Canada MDR_19A shows that residues 237-238 are in the middle of a long loop, between β strands 10 and 11, with relatively high B-factors, and R216 is also in a loop between β strand 9 and helix 6 (Figure 3A). With two missing amide ¹H and amide ¹⁵N assignments and 12 prolines, 99.3% of all possible amide ¹H and ¹⁵N atoms are assigned in both the apo and holo states. 99.6% of all possible ¹³C', ¹³C α , and ¹³C β atoms are assigned in the apo form, and 100% of all possible ¹³C', ¹³C α , and ¹³C β atoms are assigned in the holo form.

Chemical shifts were analyzed for indications of secondary structure using TALOSN (Shen and Bax 2014). The results, shown in Figure 3B-C, are in good agreement with the existing crystal structure of the apo form of PiuA (PDB 4JCC). As expected, the secondary structure regions for apo and holo PiuA are nearly identical. The only differences are a slightly increased likelihood of β -strand in residues 232-234, as if Fe(III) coordination by H238 induces a β -hairpin in the relatively flexible loop formed by residues 231-243, and perhaps two residues unwinding from the N-terminus of α 3, as R126 is likely to interact electrostatically with the siderophore (Wilde et al. 2017). F217 also may open up from α 7 upon ligand binding. All chemical shifts have been deposited in the BioMagResBank (<http://www.bmrb.wisc.edu>) under accession number 28056 (apo) and 28057 (holo).

References

- Andreini C, Putignano V, Rosato A, Banci L (2018) The human iron-proteome. *Metallomics* 10:1223–1231. <https://doi.org/10.1039/c8mt00146d>
- Cheng W, Li Q, Jiang YL, Zhou CZ, Chen Y (2013) Structures of *Streptococcus pneumoniae* PiaA and Its Complex with Ferrichrome Reveal Insights into the Substrate Binding and Release of High Affinity Iron Transporters. *PLoS One* 8: e71451. <https://doi.org/10.1371/journal.pone.0071451>
- Chu BCH, Otten R, Krewulak KD, Mulder FAA, Vogel HJ (2014) The solution structure, binding properties, and dynamics of the bacterial siderophore-binding protein FepB. *J Biol Chem* 289:29219–34. <https://doi.org/10.1074/jbc.M114.564021>
- de Boer M, Gouridis G, Vietrov R, Begg SL, Schuurman-Wolters GK, Husada F, Eleftheriadis N, Poolman B, McDevitt CA, Cordes T (2019) Conformational and dynamic plasticity in substrate-binding proteins underlies selective transport in ABC importers. *Elife* 8: e44652. <https://doi.org/10.7554/eLife.44652>
- Delaglio F, Grzesiek S, Vuister GW, Pfeifer J, Bax A (1995) NMRPipe: A multidimensional spectral processing system based on UNIX pipes. *J Biomol NMR* 6:277–293.
- Delepelaire P (2019) Bacterial ABC transporters of iron containing compounds. *Res Microbiol* 170:345–357. <https://doi.org/10.1016/j.resmic.2019.10.008>
- Hood MI, Skaar EP (2012) Nutritional immunity: Transition metals at the pathogen-host interface. *Nat. Rev. Microbiol.* 10:525–537.
- Hyberts SG, Milbradt AG, Arthanari H, Wagner G (2012) Application of iterative soft thresholding for fast reconstruction of NMR data non-uniformly sampled with multidimensional Poisson Gap scheduling. *J Biomol NMR* 52:315–327.
- Hyberts SG, Takeuchi K, Wagner G (2010) Poisson-gap sampling and forward maximum entropy reconstruction for enhancing the resolution and sensitivity of protein NMR data. *J Am Chem Soc* 132:2145–2147.
- Keller RLJ, Wüthrich K (2004) Computer-aided resonance assignment (CARA). Cantina Verlag, Goldau
- Lanie JA, Ng WL, Kazmierczak KM, Andrzejewski TM, Davidsen TM, Wayne KJ, Tettelin H, Glass JI, Winkler ME (2007) Genome sequence of Avery's virulent serotype 2 strain D39 of *Streptococcus pneumoniae* and comparison with that of unencapsulated laboratory strain R6. *J Bacteriol* 189:38–51. <https://doi.org/10.1128/JB.01148-06>
- Lee W, Tonelli M, Markley JL (2015) NMRFAM-SPARKY: Enhanced software for biomolecular NMR spectroscopy. *Bioinformatics* 31:1325–1327. <https://doi.org/10.1093/bioinformatics/btu830>
- Lynch JP, Zhanel GG (2010) *Streptococcus pneumoniae*: epidemiology and risk factors, evolution of antimicrobial resistance, and impact of vaccines. *Curr Opin Pulm Med* 16:217–225. <https://doi.org/10.1097/MCP.0b013e3283385653>
- Maciejewski MW, Schuyler AD, Gryk MR, Moraru II, Romero PR, Ulrich EL, Eghbalian HR, Livny M, Delaglio F, Hoch JC (2017) NMRbox: A Resource for Biomolecular NMR Computation. *Biophys J* 112:1529–1534. <https://doi.org/10.1016/j.bpj.2017.03.011>
- Peroutka RJ, Orcutt SJ, Strickler JE, Butt TR (2011) SUMO fusion technology for enhanced protein expression and purification in prokaryotes and eukaryotes. *Methods Mol Biol* 705:15–30. https://doi.org/10.1007/978-1-61737-967-3_2
- Raines DJ, Moroz O V, Wilson KS, Duhme-Klair A-K (2013) Interactions of a Periplasmic

- Binding Protein with a Tetradentate Siderophore Mimic. *Angew Chemie Int Ed* 52:4595–4598. <https://doi.org/10.1002/anie.201300751>
- Salzmann M, Wider G, Pervushin K, Senn H, Wüthrich K (1999) TROSY-type triple-resonance experiments for sequential NMR assignments of large proteins. *J Am Chem Soc* 121:844–848. <https://doi.org/10.1021/ja9834226>
- Shen Y, Bax A (2014) Protein structural information derived from NMR chemical shift with the neural network program TALOS-N. In: *Artificial Neural Networks: Second Edition*. Springer New York, pp 17–32.
- Wilde EJ, Hughes A, Blagova E V, Moroz O V, Thomas RP, Turkenburg JP, Raines DJ, Duhme-Klair AK, Wilson KS (2017) Interactions of the periplasmic binding protein CeuE with Fe(III) n-LICAM 4- siderophore analogues of varied linker length. *Sci Rep* 7:1–14. <https://doi.org/10.1038/srep45941>
- Zhang Y, Sen S, Giedroc D (2020) Iron Acquisition by Bacterial Pathogens: Beyond tris-Catecholate Complexes. *ChemBioChem* cbic.201900778. <https://doi.org/10.1002/cbic.201900778>

Figure Legends

Figure 1 2D ^1H - ^{15}N TROSY spectrum of apo PiuA, annotated with the backbone assignments. The assignments are labeled with the one-letter amino acid code and residue number of full-length PiuA. The TROSY spectrum was collected at 600 MHz ^1H frequency. The crowded region at the center is shown in expanded view in the lower right, and the tryptophan sidechain region is shown in the inset in the upper left.

Figure 2 2D ^1H - ^{15}N TROSY spectrum of PiuA in complex with Ga(III) and 4-LICAM, annotated with the backbone assignments. The assignments are labeled with the one-letter amino acid code and residue number of full-length PiuA. The TROSY spectrum was collected at 600 MHz ^1H frequency. The crowded region at the center is shown in expanded view in the lower right, and the tryptophan sidechain region is shown in the inset in the upper left.

Figure 3 A) Sequence alignment of *S. pneumoniae* D39 PiuA studied here by NMR with the previously solved crystal structure (PDB 4JCC) of *S. pneumoniae* Canada MDR_19A in the apo form. The four residues that are different are highlighted in a red background. Secondary structures from the crystal structure are shown above. B) Chemical-shift derived secondary structure assignments of apo and holo PiuA are painted onto the ribbon representation of the crystal structure. Where assignments are identical for apo and holo forms, helices are painted blue and beta strands red. Magenta indicates residues in beta strand conformation only in the holo form, while cyan indicates residues in alpha helical conformation only in the apo form. Sidechains are depicted as spheres for those residues that differ between strains. C) Chart of chemical-shift derived secondary structure predictions for apo (open bars) and holo (filled bars) PiuA, showing only subtle differences upon ligand binding.

Figure 1

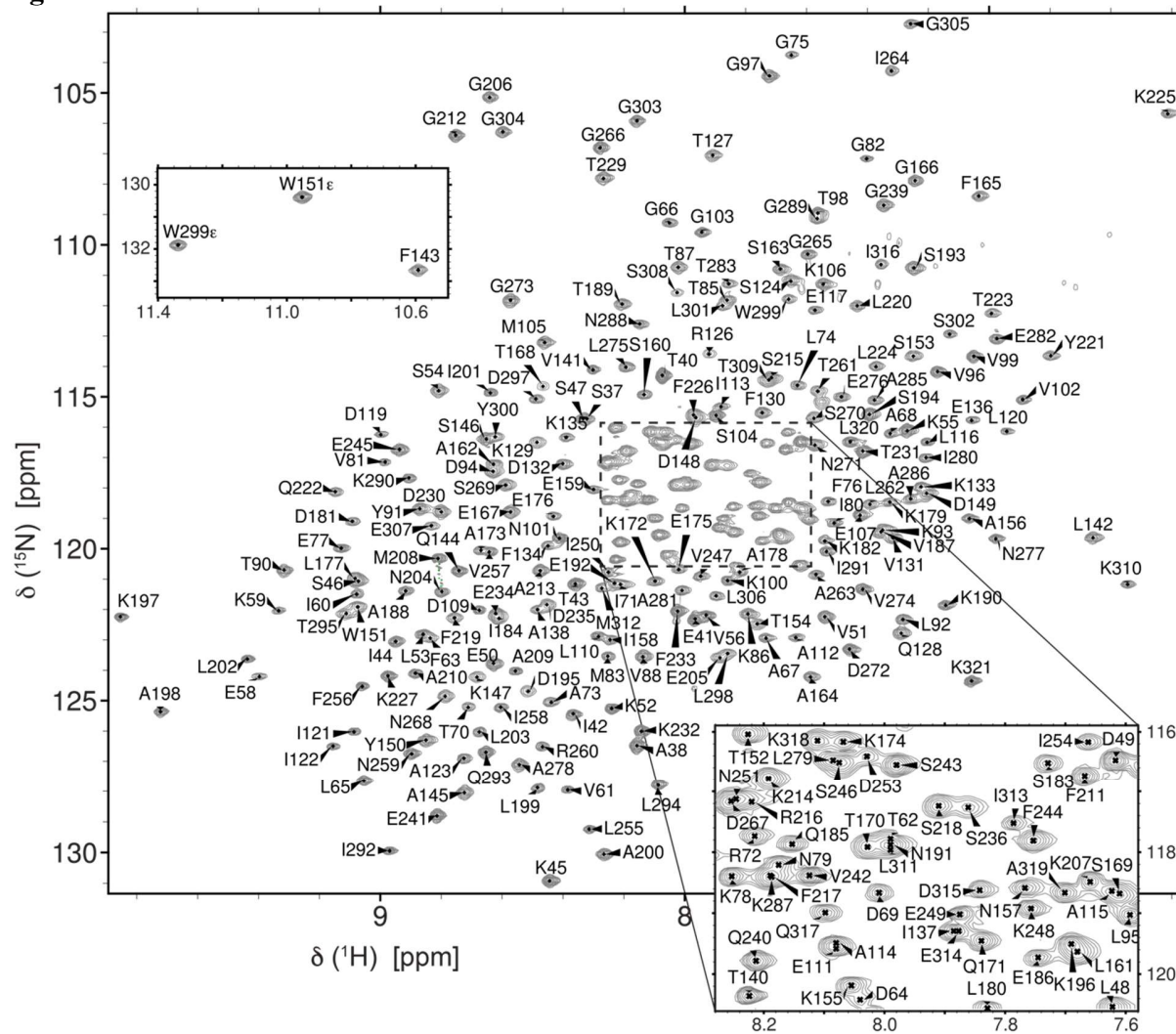


Figure 2

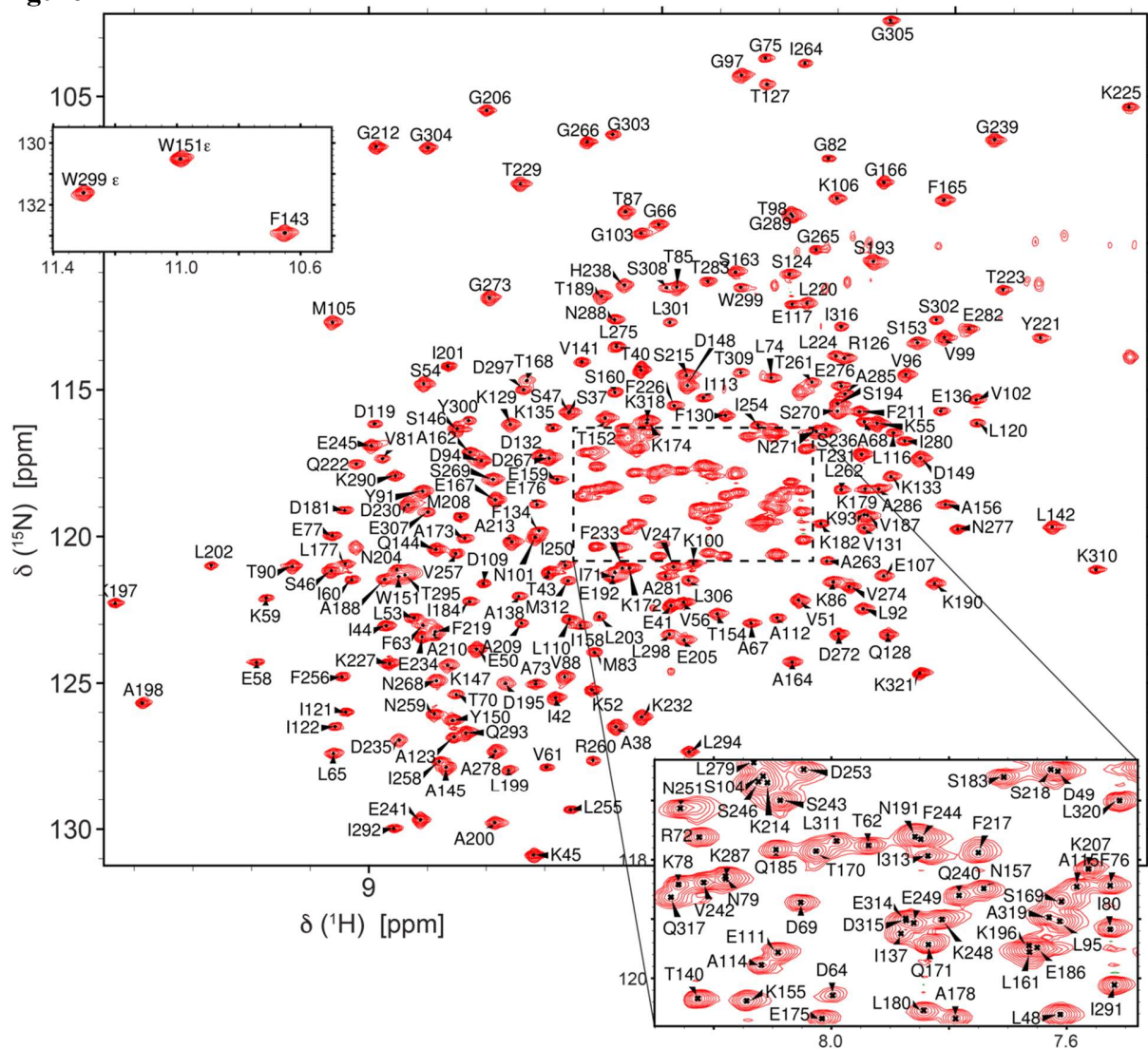


Figure 3

